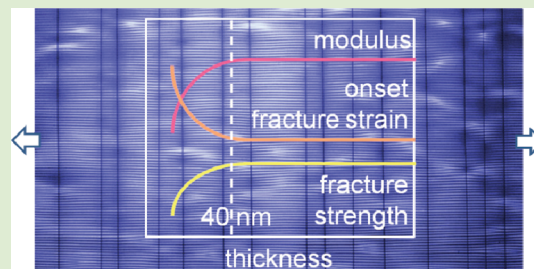


Effect of Confinement on Stiffness and Fracture of Thin Amorphous Polymer Films

Jung-Hyun Lee,[†] Jun Young Chung,[†] and Christopher M. Stafford*

Polymers Division, National Institute of Standards and Technology, 100 Bureau Drive, Gaithersburg, Maryland 20899, United States

ABSTRACT: The elastic modulus, fracture strength, and onset fracture strain of supported glassy polystyrene films with a thickness ranging from 250 to 9 nm were quantitatively determined by a recently developed wrinkling–cracking method. Films with a thickness below about 40 nm showed a decrease in both elastic modulus and fracture strength with decreasing film thickness, whereas the onset fracture strain was shown to increase. The observed variations in mechanical properties with respect to the bulk counterparts support the notion that a mechanically soft thin layer having a loosely entangled chain network exists in the near-surface region of polymeric materials, whose contribution becomes more pronounced in thinner films.



Confined polymer films are ubiquitous elements in emerging technologies ranging from flexible electronics to energy harvesting, seawater desalination, and biomedical engineering.^{1–4} The mechanical properties and stability of these elements subjected to mechanical, thermal, and/or hygroscopic load are critical considering that these characteristics signify limitations to their practical use. Stiffness (or elasticity), strength, and ductility are three of the most fundamental mechanical characteristics of a material, which are represented by its Young's modulus, tensile strength, and elongation at break.^{5–7} These three descriptors together can provide the full spectrum of mechanical behavior and thus predict the mechanical robustness of polymeric materials and thin-film devices.

There is recent theoretical and experimental evidence that confinement has a profound influence on the mechanical properties of polymer films.^{8–12} It has been reported that ultrathin (<100 nm) films of polystyrene (PS) exhibit a markedly reduced elastic modulus compared to the corresponding bulk material.^{8–10} The magnitude of this shift increases with decreasing film thickness, a phenomenon that is similar to the changes in the glass transition temperature (T_g)^{13–15} and relaxation dynamics.¹⁶ There is now a fairly general consensus that the presence of a highly mobile layer near the free surface—often loosely referred to as a “liquid-like” layer—can lead to such a significant change in thin-film properties.¹⁷ On the basis of this recognition, a two-layer model has been applied to explain the observed thickness-dependent elastic modulus of ultrathin PS films.¹⁰ Compared to studies on elastic modulus, there are relatively few studies investigating the strength and ductility of these films. The available studies of ultrathin PS films, while qualitative in nature, suggest that these films exhibit a lower tensile strength¹¹ and higher failure strain under tension¹² than those found for bulk PS.

Despite considerable efforts, however, our understanding of the mechanical behavior of confined polymer films is still not

satisfactory, in part due to intrinsic measurement challenges at the nanoscale. In addition, available methodologies are often inadequate to measure simultaneously all three mechanical properties in relevant conditions and can only permit some limited qualitative information. Using a recently developed wrinkling–cracking method,¹⁸ we report here the first comprehensive measurements of the three fundamental mechanical properties of polymer films in confined geometries. This method takes advantage of two unique instability phenomena—surface wrinkling^{19,20} and thin-film cracking^{21–23}—which occur during mechanical stretching of a flexible elastic foundation on which a thin stiff film is attached. The characteristic length scales of the resulting patterns formed on the supported thin film can be directly related to elastic modulus, fracture strength, and onset fracture strain of the film (the latter two analogous to tensile strength and elongation at break for a bulk material). In this work, we employ this approach to understand how confinement affects the mechanical properties of polymeric materials, and as shown below, our measurements provide a near-comprehensive description of the mechanical behavior of confined polymer films.

Certain commercial materials and equipment are identified in the paper to adequately specify the experimental details. In no case does such identification imply recommendation by the National Institute of Standards and Technology, nor does it imply that the material or equipment identified is necessarily the best available for the purpose. In all figures, error bars represent one standard deviation of the data, which is taken as the experimental uncertainty of the measurement.

Thin PS films supported by a poly(dimethylsiloxane) (PDMS) substrate were used as the model materials system

Received: September 23, 2011

Accepted: November 21, 2011

Published: November 28, 2011

in this study. PS ($M_w = 654$ kg/mol, $M_w/M_n = 1.09$, where M_w is the mass-average and M_n is the number-average molecular mass; Polymer Source) was used as received, and films were prepared by spin-casting from dilute solutions in toluene onto cleaned silicon wafers. The film thickness, ranging from 250 to 9 nm, was controlled by varying the solution concentration at a fixed spin speed and measured by X-ray reflectivity (X'pert Diffractometer, Phillips). Most films were used without thermal annealing, unless stated otherwise. For comparison, some films were annealed at 155 °C (50 °C above bulk T_g of PS) for 7 d and then slowly cooled. PDMS (Sylgard 184, Dow Chemical Co.) with a thickness ≈ 2.5 mm was prepared as described previously.²⁴ The Young's modulus of PDMS was determined to be (1.8 ± 0.1) MPa by a texture analyzer (model TAXT2i, Texture Technologies), and its Poisson's ratio was approximated as 0.5. To prepare PS-coated PDMS samples (PS/PDMS), the spin-coated PS films were transferred from silicon wafers onto PDMS via a water immersion technique.²⁰ Samples were then dried under ambient conditions for ≈ 10 d prior to the test.

A schematic of the wrinkling–cracking method is depicted in Figure 1a. PS/PDMS was mounted onto a strain stage

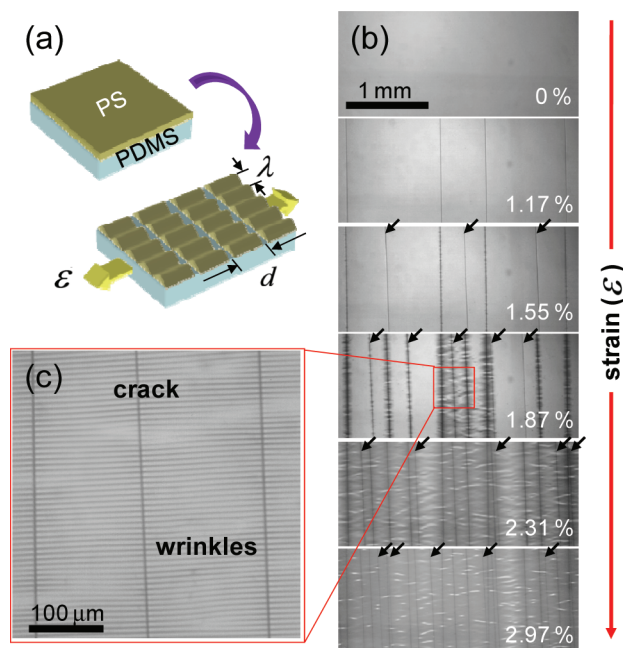


Figure 1. (a) Schematic representation of wrinkling and cracking of a thin PS film supported on a PDMS substrate under nominally uniaxial tension. ϵ , λ , and d denote applied tensile strain, wrinkle wavelength, and crack spacing, respectively. (b) Optical microscopy images of surface patterns formed on the 130 nm thick PS film as a function of ϵ . The arrows indicate newly initiated cracks between images. (c) Magnified images of the selected area illustrating the coexistence of cracks and wrinkles.

equipped with a mechanical actuator,²⁰ and then a uniaxial tensile strain was applied in a stepwise manner with a strain interval of $\approx 0.2\%$ with the strain rate of $\approx 0.1\%/s$. At each stepwise increment, surface images were taken either by an optical microscope (for films > 50 nm; Labophot-2, Nikon) or an optical profilometer (for films < 50 nm; NewView 7300, Zygo) after waiting ≈ 2 min to avoid possible time- (or rate-) dependent effects.²⁵ The images that displayed a change in crack density were used for data analysis. All tests were

conducted at room temperature, well below T_g of the bulk PS, and within the small-strain regime ($< 3\%$) where PS and PDMS are known to exhibit linear elastic behavior.^{8,20,26} Figure 1b shows the evolution of surface patterns on PS/PDMS as a function of the applied strain (ϵ). Upon stretching, the film undergoes fracture with regularly spaced parallel cracks aligned perpendicular to the stretching direction. New cracks form in the middle of the pre-existing fracture segment, and the crack density, defined as the reciprocal of the average crack spacing ($\langle d \rangle$), increases with strain (Figure 1b). Together with thin-film cracking, sinusoidal wrinkling patterns with a well-defined wavelength (λ) begin to emerge at slightly higher strains, which are caused by a lateral Poisson contraction orthogonal to the stretching direction. The coexistence of thin-film cracks and surface wrinkles is typically observed at strains $> 1.5\%$ (Figure 1c). Note that the sequence of instability events is determined by the difference in the onset strain between cracking and wrinkling and depends on constituent material property combination, such as film toughness, elastic mismatch, and so forth.^{24,27–29} The exact dependence is complex, but in general, cracking occurs first for brittle polymers (e.g., PS), whereas wrinkling occurs first for ductile or relatively tough ones (e.g., polyamide).¹⁸

The mechanism of thin-film cracking has been well-established in the literature.^{21–23} It has been shown that the cracking mechanism is governed by the bisection of each fragment at its midpoint when the crack spacing becomes shorter than the critical length ($d_c = 4h_f E_f / E_s$). Here, h_f is the film thickness, E is the elastic modulus, and the subscript f and s denote the film and substrate, respectively. In this bisection regime of thin-film cracking, the average crack density can be described by $1/\langle d \rangle = E_s(\epsilon - \epsilon^*)/2h_f \sigma_f^*$, where σ_f^* and ϵ^* are the fracture strength and onset fracture strain of the film, respectively.^{18,22} This model assumes small-strain linear elasticity and considers that the stress field across the fragment is given by $\sigma_f = \sigma_{f,\max}[1 - (2x/d)^2]^{1/2}$, where the maximum occurs at $x = 0$ (midpoint) and the minimum at $x = \pm d/2$ (both edges) and that new cracks initiate at a critical stress level (i.e., $\sigma_{f,\max} = \sigma_f^*$). This model also assumes the perfect adhesion at the film–substrate interface. No noticeable delamination or blistering at the PS–PDMS interface was observed in the small-strain regime used in this study, thus validating the applicability of the model to our system. Bisection cracking continues until other dissipative processes (e.g., interfacial delamination/slippage, viscoelasticity) take place within the material system, leading to a progressive diminution of the stress level transferred from the substrate to the film.^{21,23}

In this work, we consider only the bisection regime of the thin-film cracking described above, where crack density is linearly proportional to applied strain. Figure 2a shows the average crack density plotted against strain, indicating the linear dependence of the crack density on strain. The best linear fit to the crack density versus strain plot allows the determination of the fracture strength and onset fracture strain from the slope and the intercept to zero crack density, respectively, using the relation: $1/\langle d \rangle = (E_s/2h_f \sigma_f^*)(\epsilon - \epsilon^*)$. There are some studies^{28,29} indicating that onset fracture strain depends on the elastic mismatch between the film and the substrate. It should be noted, however, that onset fracture strain is insensitive to the material system as long as the quantity E_s/E_f is sufficiently small (< 0.001), which is satisfied in our case (i.e., $E_s \approx O(1)$ MPa; $E_f \approx O(1)$ GPa). This was also confirmed by earlier experimental work.³⁰

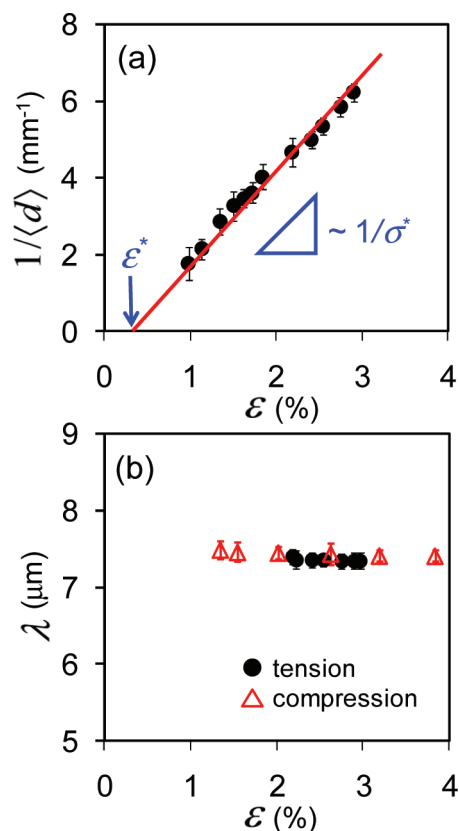


Figure 2. Cracking and wrinkling behavior of a 130 nm thick PS film. (a) Plot of inverse crack density ($1/\langle d \rangle$) vs strain (ϵ). Fracture strength (σ^*) and onset fracture strain (ϵ^*) can be deduced from the slope and x -intercept of the linear regression line as described in the text. (b) Wrinkle wavelength (λ) as a function of ϵ under tension (circles) and compression (triangles).

Based on wrinkling mechanics,¹⁹ the Young's modulus of a film can be determined from the wrinkle wavelength by $\hat{E}_f = 3\hat{E}_s(\lambda/2\pi h_f)^3$, where $\hat{E} = E(1 - \nu^2)$ is the plane-strain modulus and ν is Poisson's ratio. While many of previous works have utilized compression-induced wrinkling to measure film modulus,¹⁹ the wrinkling patterns in our approach develop in the presence of cracks under nominally uniaxial tension. To assess how pre-existing cracks and different loading modes might affect wrinkling patterns, we compared the wrinkle wavelengths measured under two different loading modes: tension (with cracks) and compression (without cracks). As shown in Figure 2b, it is clear that the two sets of data do not show any appreciable difference. In addition, the wavelengths remain nearly constant within the range of strains tested. These results indicate that the presence of cracks, type of loading mode, and level of applied strain have negligible effects on the wrinkle wavelength, thus providing confidence in the current approach as well as the final results.

Using this approach, the present study aimed to elucidate how confinement (tuned by varying film thickness) affects the mechanical properties of thin polymer films. We first evaluated the mechanical properties of the two representative PS films having very different thicknesses: 140 nm vs 8.6 nm. We chose these film thicknesses to assess whether fracture strength and onset fracture strain vary in a manner similar to the variation in elastic modulus observed in previous studies^{8,10} (i.e., a decrease in modulus with a decrease in film thickness below ≈ 40 nm).

Consistent with previous data,¹⁰ the measured moduli (\hat{E}_f) for the thicker and thinner films were significantly different [(5.40 ± 0.22) GPa and (1.79 ± 0.22) GPa, respectively]. Figure 3

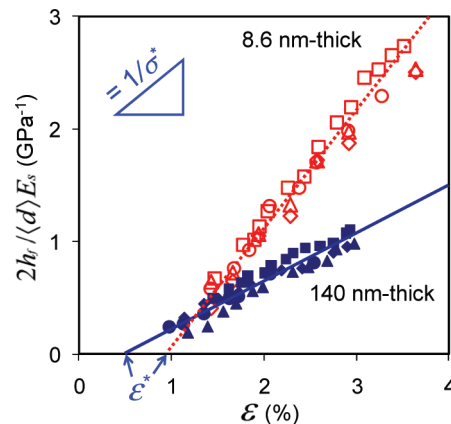


Figure 3. Rescaled crack density ($2h_f/\langle d \rangle E_s$) as a function of strain (ϵ) for 8.6 nm thick (open symbols) and 140 nm thick (closed symbols) PS films, demonstrating lower fracture strength but higher onset fracture strain for the thinner film. Each symbol represents the data set obtained from different samples.

displays the plots of rescaled crack density ($2h_f/\langle d \rangle E_s$) versus strain for these films. On one hand, the rate of crack growth (i.e., slope of the data) for the thinner film was much faster than that for the thicker film, implying less resistance to fracture. The fracture strength of the 8.6 nm thick film was (9.9 ± 0.8) MPa, while that of the 140 nm thick film was (21.3 ± 2.9) MPa. On the other hand, the onset fracture strain for the thinner film was found to be $(0.79 \pm 0.27)\%$, which was more than twice that for the thicker film, $(0.35 \pm 0.23)\%$. Films prepared under different processing and annealing conditions may exhibit different mechanical properties due to residual stress effects.³¹ We examined two identical PS films with and without thermal annealing at 155°C ($>T_g$) for 7 days but found no marked disparities in the mechanical properties for both films.

To further determine the transition thickness at which the film properties begin to deviate from their bulk values, data were obtained for the modulus, fracture strength, and onset fracture strain of PS films with thicknesses ranging from 250 to 9 nm (see Figure 4). Interestingly, all of the mechanical properties examined here were observed to have a similar transition thickness (≈ 40 nm). For films >40 nm, a plateau is present. We found that the obtained plateau values of plane-strain modulus (≈ 5.0 GPa), fracture strength (≈ 21 MPa), and onset fracture strain ($\approx 0.4\%$) bear close resemblance to their bulk counterparts reported in the literature (plane-strain modulus, ≈ 4.5 GPa; tensile strength, ≈ 30 MPa; elongation at break, $\approx 1\%$).¹⁸ For films less than 40 nm, their elastic modulus and fracture strength decrease progressively with a decrease in thickness, while their onset fracture strain, although there is a degree of scatter in the data, is greater for the thinner films. Substrate clamping effects may cause some variation in the estimate of onset fracture strain. Nevertheless, the calculations using the elastic-perfectly brittle constitutive model,⁶ which provides a good approximation for the strain for brittle polymers (i.e., $\sigma^*/\hat{E}_f \approx \epsilon^*$), showed satisfactory agreement with measurement as demonstrated in Figure 4c.

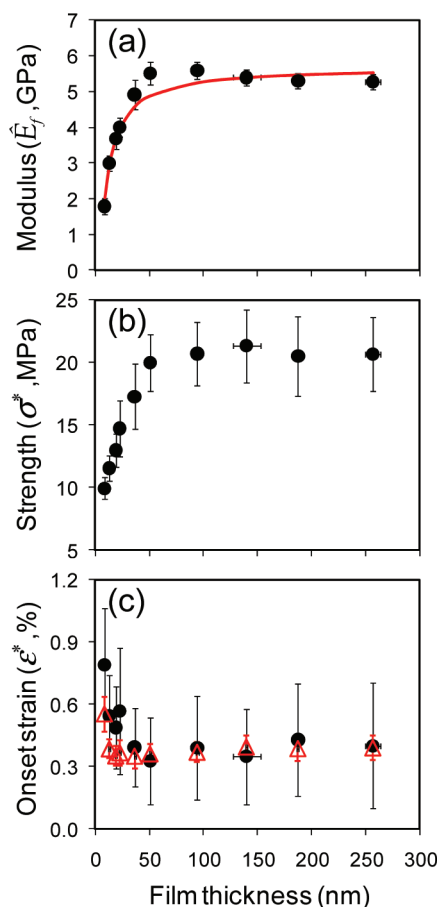


Figure 4. Mechanical properties of thin PS films plotted against film thickness. (a) Plane-strain modulus (\hat{E}_t). The solid line is a best fit to the data using the two-layer model (see ref 10 for details). (b) Fracture strength (σ^*). (c) Onset fracture strain (ϵ^*) (circles: experimental data; triangles: estimated values calculated by σ^*/\hat{E}_t using the measured values of σ^* and \hat{E}_t). Error bars indicate the standard deviation of measurements on at least five samples for each thickness.

The mechanical properties of polymer materials are closely related to their molecular structures such as segmental mobility and density. Previous studies have shown that the presence of a high mobility layer in the vicinity of the polymer surface was accountable for the apparent suppression in the modulus and T_g of ultrathin polymer films.^{8,10,13} Similar to a previous work,¹⁰ we found that the generic two-layer model, although there is evidence of a more complex heterogeneous structure in nanoconfined polymers,^{32,33} could effectively produce a good fit to the measured modulus data, yielding a thickness of 2.6 nm and modulus of 0.1 GPa for the surface layer (solid line in Figure 4a). In addition, it has been suggested on the basis of the chain packing theory that the fraction of intermolecular entanglements is significantly reduced near the free surface due to a reduction in the volume pervaded by a polymer chain at the interface.³⁴ This has been further supported by experimental evidence pointing to enhanced deformation of strained, freestanding PS thin films.¹² The results shown in Figure 4 support this notion and allow us to gain insights into the structural nature of the surface layer. A decrease in intermolecular entanglement density near the free surface would enhance the segmental mobility but reduce the strength of intermolecular forces; thereby one would expect that the elastic modulus and fracture strength of ultrathin polymer films

would decrease with a decrease in film thickness. Such a poorly entangled and thus highly mobile chain network can also effectively relieve built-up stress during deformation before reaching the critical value of fracture as evidenced by previous simulation work,⁸ which corroborates our results on the onset fracture strain. The increase in the onset fracture strain for thinner films could be further supported by the idea of the loss of plastic constraint at the free polymer surface.^{35,36} Our results of increased ductility upon confinement appear contrary to simulation results that indicate that packing frustration is relieved upon confinement,³⁷ which would lead to stiffening and potentially embrittlement of the films. Conversely, the interpretation of the results of our study is in line with a recent study reporting similar mechanical behavior of confined PS thin films under indentation.³⁸

In conclusion, we reported a detailed study on the change in mechanical properties of supported thin polymer films with thickness variation, which provided insights into the structural nature of polymeric materials at the polymer–air interface. Experimental results indicated that the PS films become less stiff, less strong, but more ductile with decreasing film thickness below approximately 40 nm. The observed thickness-dependent mechanical behavior supports the notion that there exists a few nanometer thick, mechanically soft layer near the free surface which is composed of a loosely entangled chain network. Our findings will have important implications for applications that feature polymer films in confined geometries, such as flexible electronics, fuel cells, photovoltaics, and water/gas separation membranes, as well as artificial skin.

AUTHOR INFORMATION

Corresponding Author

*E-mail: chris.stafford@nist.gov.

Author Contributions

†These authors contributed equally.

Notes

The authors declare no competing financial interest.

ACKNOWLEDGMENTS

The authors thank Dr. Hae-Jeong Lee for X-ray reflectivity measurements.

REFERENCES

- (1) Forrest, S. R. *Nature* **2004**, *428*, 911.
- (2) Borup, R.; Meyers, J.; Pivovar, B.; Kim, Y. S.; Mukundan, R.; Garland, N.; Myers, D.; Wilson, M.; Garzon, F.; Wood, D.; et al. *Chem. Rev.* **2007**, *107*, 3904.
- (3) Geise, G. M.; Lee, H.-S.; Miller, D. J.; Freeman, B. D.; McGrath, J. E.; Paul, D. R. *J. Polym. Sci., Part B: Polym. Phys.* **2010**, *48*, 1685.
- (4) Someya, T.; Sekitani, T.; Iba, S.; Kato, Y.; Kawaguchi, H.; Sakurai, T. *Proc. Natl. Acad. Sci. U.S.A.* **2004**, *101*, 9966.
- (5) Gordon, J. E. *The New Science of Strong Materials*; Princeton University Press: Princeton, NJ, 1968.
- (6) Seitz, J. T. *J. Appl. Polym. Sci.* **1993**, *49*, 1331.
- (7) Wong, E. W.; Sheehan, P. E.; Lieber, C. M. *Science* **1997**, *277*, 1971.
- (8) Bohme, T. R.; de Pablo, J. J. *J. Chem. Phys.* **2002**, *116*, 9939.
- (9) Zhao, J. H.; Kiene, M.; Hu, C.; Ho, P. S. *Appl. Phys. Lett.* **2000**, *77*, 2843.
- (10) Stafford, C. M.; Vogt, B. D.; Harrison, C.; Julthongpipit, D.; Huang, R. *Macromolecules* **2006**, *39*, 5095.
- (11) Wang, Y.; Bhushan, B.; Zhao, X. *Nanotechnology* **2009**, *20*, 045301.

- (12) Si, L.; Massa, M. V.; Dalnoki-Veress, K.; Brown, H. R.; Jones, R. A. L. *Phys. Rev. Lett.* **2005**, *94*, 127801.
- (13) Keddie, J. L.; Jones, R. A. L.; Cory, R. A. *Europhys. Lett.* **1994**, *27*, 59.
- (14) Forrest, J. A.; Dalnoki-Veress, K. *Adv. Colloid Interface Sci.* **2001**, *94*, 167.
- (15) Alcoutlabi, M.; McKenna, G. B. *J. Phys.: Condens. Matter* **2005**, *17*, R461.
- (16) Fakhraei, Z.; Forrest, J. A. *Science* **2008**, *319*, 600.
- (17) Keddie, J. L.; Jones, R. A. L.; Cory, R. A. *Faraday Discuss.* **1994**, *98*, 219.
- (18) Chung, J. Y.; Lee, J. H.; Beers, K. L.; Stafford, C. M. *Nano Lett.* **2011**, *11*, 3361.
- (19) Chung, J. Y.; Nolte, A. J.; Stafford, C. M. *Adv. Mater.* **2011**, *23*, 349.
- (20) Stafford, C. M.; Harrison, C.; Beers, K. L.; Karim, A.; Amis, E. J.; VanLandingham, M. R.; Kim, H.-C.; Volksen, W.; Miller, R. D.; Simonyi, E. E. *Nat. Mater.* **2004**, *3*, 545.
- (21) Volynskii, A. L.; Panchuk, D. A.; Moiseeva, S. V.; Keckek'yan, A. S.; Dement'ev, A. I.; Yarysheva, L. M.; Bakeev, N. F. *Russ. Chem. Bull.* **2009**, *58*, 865.
- (22) Bazhenov, S. L.; Volynskii, A. L.; Alexandrov, V. M.; Bakeev, N. F. *J. Polym. Sci., Part B: Polym. Phys.* **2002**, *40*, 10.
- (23) Spolenak, R.; Heinrich, M.; Gruber, P.; Orso, S.; Handge, U. A. *Nano Lett.* **2006**, *6*, 2026.
- (24) Chung, J. Y.; Chastek, T. Q.; Fasolka, M. J.; Ro, H. W.; Stafford, C. M. *ACS Nano* **2009**, *3*, 844.
- (25) Efimenko, K.; Rackaitis, M.; Manias, E.; Vaziri, A.; Mahadevan, L.; Genzer, J. *Nat. Mater.* **2005**, *4*, 293.
- (26) Chung, J. Y.; Youngblood, J. P.; Stafford, C. M. *Soft Matter* **2007**, *3*, 1163.
- (27) Beuth, J. L. Jr. *Int. J. Solids Struct.* **1992**, *29*, 1657.
- (28) Douville, N. J.; Li, Z.; Takayama, S.; Thouless, M. D. *Soft Matter* **2011**, *7*, 6493.
- (29) Waller, J. H.; Lalande, L.; Leterrier, Y.; Manson, J.-A. E. *Thin Solid Films* **2011**, *519*, 4249.
- (30) Li, T.; Huang, Z.; Suo, Z.; Lacour, S. P.; Wagner, S. *Appl. Phys. Lett.* **2004**, *85*, 3435.
- (31) Reiter, G.; Napolitano, S. *J. Polym. Sci., Part B: Polym. Phys.* **2010**, *48*, 2544.
- (32) Ellison, C. J.; Torkelson, J. M. *Nat. Mater.* **2003**, *2*, 695.
- (33) Bansal, A.; Yang, H.; Li, C.; Cho, K.; Benicewicz, B. C.; Kumar, S. K.; Schadler, L. S. *Nat. Mater.* **2005**, *4*, 693.
- (34) Brown, H. R.; Russell, T. P. *Macromolecules* **1996**, *29*, 798.
- (35) Donald, A. M.; Chan, T.; Kramer, E. J. *J. Mater. Sci.* **1981**, *16*, 669.
- (36) Chan, T.; Donald, A. M.; Kramer, E. J. *J. Mater. Sci.* **1981**, *16*, 676.
- (37) Riggelman, R. A.; Yoshimoto, K.; Douglas, J. F.; de Pablo, J. J. *Phys. Rev. Lett.* **2006**, *97*, 045502.
- (38) Rowland, H. D.; King, W. P.; Pethica, J. B.; Cross, G. L. W. *Science* **2008**, *322*, 720.